International Journal of Engineering Science 84 (2014) 11–17

Contents lists available at ScienceDirect

International Journal of Engineering Science

journal homepage: www.elsevier.com/locate/ijengsci

A conservative Allen–Cahn equation with a space–time dependent Lagrange multiplier

Junseok Kim [a], Seunggyu Lee [a], Yongho Choi [a,*]

[a] Department of Mathematics, Korea University, Seoul 136-713, Republic of Korea

ARTICLE INFO

Article history:
Received 11 January 2014
Received in revised form 9 May 2014
Accepted 7 June 2014

Keywords:
Allen–Cahn equation
Operator splitting
Mass conservation
Multigrid method
Finite difference method

ABSTRACT

We present a new numerical scheme for solving a conservative Allen–Cahn equation with a space–time dependent Lagrange multiplier. Since the well-known classical Allen–Cahn equation does not have mass conservation property, Rubinstein and Sternberg introduced a nonlocal Allen–Cahn equation with a time dependent Lagrange multiplier to enforce conservation of mass. However, with their model it is difficult to keep small features since they dissolve into the bulk region. One of the reasons for this is that mass conservation is realized by a global correction using the time-dependent Lagrange multiplier. To resolve the problem, we use a space–time dependent Lagrange multiplier to preserve the volume of the system and propose a practically unconditionally stable hybrid scheme to solve the model. The numerical results indicate a potential usefulness of our proposed numerical scheme for accurately calculating geometric features of interfaces.

1. Introduction

The Allen–Cahn (AC) equation (Allen & Cahn, 1979) was introduced originally as a phenomenological model for antiphase domain coarsening in a binary alloy:

$$\frac{\partial \phi}{\partial t}(\mathbf{x},t) = -M\left(\frac{F'(\phi(\mathbf{x},t))}{\epsilon^2} - \Delta\phi(\mathbf{x},t)\right), \quad \mathbf{x}\in\Omega, \quad t>0, \tag{1}$$

$$\mathbf{n}\cdot\nabla\phi(\mathbf{x},t) = 0, \quad \mathbf{x}\in\partial\Omega. \tag{2}$$

Here Ω, t, M, and $\mathbf{n}$ denote a bounded domain, time, a positive kinetic coefficient, and the unit outer normal vector on the domain boundary, respectively. $F(\phi) = 0.5\phi^2(1-\phi)^2$ is a double-well potential and ϵ is the gradient energy coefficient related to the interfacial energy. The quantity $\phi(\mathbf{x},t)\in[0,1]$ is an order parameter, which is one of the concentrations of the two components in a binary mixture. For example, $\phi = 1$ in the one phase and $\phi = 0$ in the other phase. The interface between two phases is defined by $\Gamma = \{\mathbf{x}\in\Omega | \phi(\mathbf{x},t) = 0.5\}$. Allen and Cahn (1979) also showed that the normal velocity v on a single closed interface Γ is governed by its mean curvature

$$v(\mathbf{x},t) = \kappa(\mathbf{x},t), \quad \mathbf{x}\in\Gamma, \tag{3}$$

* Corresponding author. Tel.: +82 2 3290 3077.
E-mail addresses: cfdkim@korea.ac.kr (J. Kim), sky509@korea.ac.kr (S. Lee), poohyongho@korea.ac.kr (Y. Choi).
URL: http://math.korea.ac.kr/~cfdkim

http://dx.doi.org/10.1016/j.ijengsci.2014.06.004
0020-7225/

where $\kappa(\mathbf{x},t)$ is the mean curvature of the interface Γ. This dynamical property has been studied in Ma, Jiang, and Xiang (2009), Brassel and Bretin (2011), Ren and Wei (2009), Ward and Wetton (2001). Fig. 1(a) and (b) show the temporal evolutions of curves with the classical AC and the conservative AC equations in two dimensions, respectively. The dashed lines are the initial curves and the solid lines are the evolutions of interfaces. The directions of evolutions are indicated by arrows. We observe that the classical AC does not conserve its initial mass, whereas the conservative AC equation does. We can check that the AC type dynamics does not preserve the volume fractions, i.e.,

$$\frac{\mathrm{d}}{\mathrm{d}t}\int_\Omega \phi \,\mathrm{d}\mathbf{x} = \int_\Omega \phi_t \,\mathrm{d}\mathbf{x} = \int_\Omega M\left(-\frac{F'(\phi)}{\epsilon^2}+\Delta\phi\right)\mathrm{d}\mathbf{x} = -\int_\Omega \frac{MF'(\phi)}{\epsilon^2}\,\mathrm{d}\mathbf{x} + \int_{\partial\Omega} M\mathbf{n}\cdot\nabla\phi \,\mathrm{d}s = -\int_\Omega \frac{MF'(\phi)}{\epsilon^2}\,\mathrm{d}\mathbf{x},$$

which is not always zero. Here, we set $M=1$ for simplicity. To preserve the volume, Rubinstein and Sternberg (1992) introduced a Lagrange multiplier $\beta(t)$ into the AC model

$$\frac{\partial\phi}{\partial t}(\mathbf{x},t) = -\frac{F'(\phi(\mathbf{x},t))}{\epsilon^2} + \Delta\phi(\mathbf{x},t) + \beta(t). \tag{4}$$

Here $\beta(t)$ must satisfy $\beta(t) = \int_\Omega F'(\phi(\mathbf{x},t))\,\mathrm{d}\mathbf{x}/(\epsilon^2\int_\Omega \mathrm{d}\mathbf{x})$ to keep the mass conservation, and this formulation has been widely used (Bates & Jin, 2013; Yang, Feng, Liu, & Shen, 2006; Zhang & Tang, 2007). The normal velocity v on a single closed interface Γ is given by the volume-preserving mean curvature flow:

$$v(\mathbf{x},t) = \kappa(\mathbf{x},t) - \frac{1}{|\Gamma|}\int_\Gamma \kappa \,\mathrm{d}s, \quad \mathbf{x}\in\Gamma, \tag{5}$$

where $|\Gamma|$ is the total curve length in two-dimensional space and the total area in three-dimensional space. Rubinstein and Sternberg's model has been studied analytically and numerically (Beneš, Yazaki, & Kimura, 2011; Brassel & Bretin, 2011; Bronsard & Stoth, 1997; Ward, 1996; Xia, Xu, & Shu, 2009; Yue, Zhou, & Feng, 2007;). However, it has a drawback on preserving small features since the Lagrange multiplier is only a function of time variable. For example, there is a critical radius of drop which eventually disappears below the radius. This phenomenon is observed in the frame of the Cahn–Hilliard model (Yue et al., 2007).

The main purpose of this article is to propose a practically unconditionally stable numerical scheme for the conservative AC equation with a space–time dependent Lagrange multiplier. The scheme is based on the recently developed hybrid scheme for the AC equation (Li, Lee, Jeong, & Kim, 2010) with an exact mass-conserving update at each time step.

The paper is organized as follows. In Section 2, we present the conservative AC equation with a space–time dependent Lagrange multiplier. A numerical algorithm using an operator splitting method is described in Section 3. Several numerical results demonstrating the accuracy and robustness of the proposed scheme are described in Section 4. Conclusions are made in Section 5.

2. Conservative Allen–Cahn equation

The authors in Brassel and Bretin (2011) proposed the following conservative AC equation which guarantees to preserve small geometric features:

$$\frac{\partial\phi(\mathbf{x},t)}{\partial t} = -\frac{F'(\phi(\mathbf{x},t))}{\epsilon^2} + \Delta\phi(\mathbf{x},t) + \beta(t)\sqrt{2F(\phi(\mathbf{x},t))}, \tag{6}$$

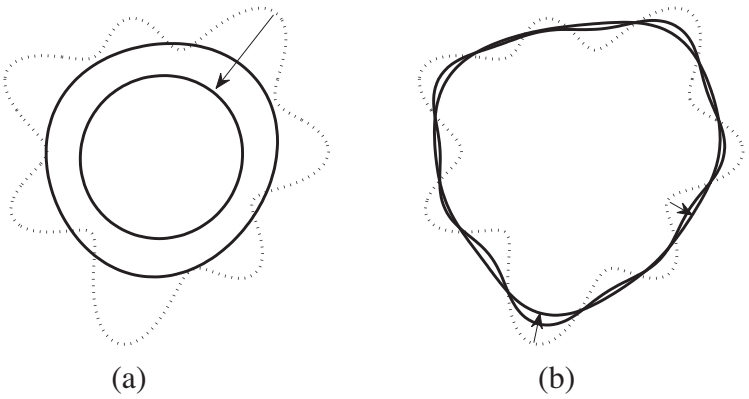

Fig. 1. Temporal evolutions of arbitrary curves with (a) the AC equation and (b) the conservative AC equation. The dashed lines are the initial curves and directions of evolutions are indicated by arrows.

where $\beta(t) = \int_\Omega F'(\phi(\mathbf{x},t))\ d\mathbf{x} / \left[\epsilon^2 \int_\Omega \sqrt{2F(\phi(\mathbf{x},t))}\ d\mathbf{x}\right]$. Then, the solution $\phi(\mathbf{x},t)$ of the conservative AC Eq. (6) possesses the total mass conservation property, i.e.,

$$\frac{d}{dt}\int_\Omega \phi\ d\mathbf{x} = \int_\Omega \phi_t\ d\mathbf{x} = \int_\Omega \left[-\frac{F'(\phi)}{\epsilon^2} + \Delta\phi + \beta(t)\sqrt{2F(\phi)}\right] d\mathbf{x} = -\frac{1}{\epsilon^2}\int_\Omega F'(\phi)\ d\mathbf{x} + \int_{\partial\Omega} \mathbf{n}\cdot\nabla\phi\ ds + \beta(t)\int_\Omega \sqrt{2F(\phi)}\ d\mathbf{x}$$
$$= -\frac{1}{\epsilon^2}\int_\Omega F'(\phi)\ d\mathbf{x} + \beta(t)\int_\Omega \sqrt{2F(\phi)}\ d\mathbf{x} = 0,$$

where we used the homogenous Neumann boundary condition (2). We note that to conserve mass, there is a classical model such as the Cahn–Hilliard equation (Abels, Garcke, & Grun, 2012; Cahn & Hilliard, 1958; Heida, Malek, & Rajagopal, 2012; Lowengrub & Truskinovsky, 1998). Also, see (Heida, Malek, & Rajagopal, 2012) on the development and generalizations of Allen–Cahn and Stefan equations within a thermodynamic framework.

3. Numerical solution algorithm

In this section, we propose a new hybrid numerical algorithm for solving the conservative AC equation. For simplicity, we consider a two-dimensional space. The three-dimensional case is defined analogously. Let a computational domain $\Omega = [a,b]\times[c,d]$ be partitioned into a uniform mesh with spatial step size $h = (b-a)/N_x = (d-c)/N_y$. Here, N_x and N_y are the numbers of cells in x- and y-directions, respectively. The center of each cell, Ω_{ij}, is located at $\mathbf{x}_{ij} = (x_i, y_j) = (a+(i-0.5)h, c+(j-0.5)h)$ for $i = 1,\dots,N_x$ and $j = 1,\dots,N_y$. Let ϕ_{ij}^n be approximations of $\phi(x_i, y_j, n\Delta t)$, where $\Delta t = T/N_t$ is the temporal step size, T is the final time, and N_t is the total number of time steps. For the zero Neumann boundary condition, we use $\nabla_d\phi_{1/2,j}^n = \nabla_d\phi_{N_x+1/2,j}^n = \nabla_d\phi_{i,1/2}^n = \nabla_d\phi_{i,N_y+1/2}^n = 0$, where $\nabla_d\phi_{i+1/2,j}^n = (\phi_{i+1,j}^n - \phi_{ij}^n)/h$. We define a discrete Laplacian operator by $\Delta_d\phi_{ij}^n = (\nabla_d\phi_{i+1/2,j}^n - \nabla_d\phi_{i-1/2,j}^n)/h$ and the discrete l^2 inner product by $(\phi,\psi)_h = h^2\sum_{i=1}^{N_x}\sum_{j=1}^{N_y}\phi_{ij}\psi_{ij}$. We also define the discrete norm as $\|\phi\|^2 = (\phi,\phi)_h$. In this paper, we use an operator splitting method, in which we numerically solve the original problem Eq. (6) by solving successively a sequence of simpler problems:

$$\phi_t = \Delta\phi, \tag{7}$$
$$\phi_t = -\frac{F'(\phi)}{\epsilon^2}, \tag{8}$$
$$\phi_t = \beta\sqrt{2F(\phi)}. \tag{9}$$

First, we solve Eq. (7) by applying the implicit Euler's method:

$$\frac{\phi_{ij}^{n+1,1} - \phi_{ij}^n}{\Delta t} = \Delta_d\phi_{ij}^{n+1,1}. \tag{10}$$

We use the multigrid method (Aristotelous, Karakashian, & Wise, 2013; Briggs & Steve, 1987; Trottenberg, Oosterlee, & Schuller, 2001) to solve the implicit discrete Eq. (10). We should note that we can use the Crank–Nicolson scheme as in Li et al. (2010) to solve Eq. (7). However, although the Crank–Nicolson scheme is unconditionally stable, it is well-known that the scheme suffers from oscillatory behavior with large time steps. Next, Eq. (8) is solved analytically using the method of separation of variables (Stuart & Humphries, 1998) and the solution is given as

$$\phi_{ij}^{n+1,2} = 0.5 - \frac{1-2\phi_{ij}^{n+1,1}}{2\sqrt{\left(1-2\phi_{ij}^{n+1,1}\right)^2 + 4\phi_{ij}^{n+1,1}\left(1-\phi_{ij}^{n+1,1}\right)e^{-\frac{\Delta t}{\epsilon^2}}}}. \tag{11}$$

Finally, we discretize Eq. (9) as

$$\frac{\phi_{ij}^{n+1} - \phi_{ij}^{n+1,2}}{\Delta t} = \beta^{n+1,2}\sqrt{2F\left(\phi_{ij}^{n+1,2}\right)}. \tag{12}$$

By Eq. (12), we get $\phi_{ij}^{n+1} = \phi_{ij}^{n+1,2} + \Delta t\beta^{n+1,2}\sqrt{2F\left(\phi_{ij}^{n+1,2}\right)}$, then by the property of mass conservation

$$\sum_{i=1}^{N_x}\sum_{j=1}^{N_y}\phi_{ij}^0 = \sum_{i=1}^{N_x}\sum_{j=1}^{N_y}\phi_{ij}^{n+1} = \sum_{i=1}^{N_x}\sum_{j=1}^{N_y}\left(\phi_{ij}^{n+1,2} + \Delta t\beta^{n+1,2}\sqrt{2F\left(\phi_{ij}^{n+1,2}\right)}\right). \tag{13}$$

Thus

$$\beta^{n+1,2} = \frac{1}{\Delta t}\sum_{i=1}^{N_x}\sum_{j=1}^{N_y}\left(\phi_{ij}^0 - \phi_{ij}^{n+1,2}\right) \Big/ \sum_{i=1}^{N_x}\sum_{j=1}^{N_y}\sqrt{2F\left(\phi_{ij}^{n+1,2}\right)}. \tag{14}$$

Now, our proposed numerical scheme can be summarized as

$$\frac{\phi_{ij}^{n+1,1}-\phi_{ij}^{n}}{\Delta t}=\Delta_d\phi_{ij}^{n+1,1}, \tag{15}$$

$$\phi_{ij}^{n+1,2}=0.5-\frac{1-2\phi_{ij}^{n+1,1}}{2\sqrt{\left(1-2\phi_{ij}^{n+1,1}\right)^2+4\phi_{ij}^{n+1,1}\left(1-\phi_{ij}^{n+1,1}\right)e^{-\frac{\Delta t}{\epsilon^2}}}}, \tag{16}$$

$$\phi_{ij}^{n+1}=\phi_{ij}^{n+1,2}+\Delta t\beta^{n+1,2}\sqrt{2F\left(\phi_{ij}^{n+1,2}\right)}. \tag{17}$$

4. Numerical results

In this section, we perform numerical experiments such as the basic mechanism of the model, a comparison with previous model, and the temporal evolution of drops in two- and three-dimensional spaces. The equilibrium order parameter $\phi=0.5(1+\tanh[x/(2\epsilon)])$ varies from 0.05 to 0.95 over a distance of approximately $4\epsilon\tanh^{-1}(0.9)$ across the interfacial regions. Therefore, if we want this value to be approximately m grid points, then ϵ value is given as $\epsilon_m=hm/[4\tanh^{-1}(0.9)]$ (Kim, 2012). Throughout the rest of the paper, we shall use ϵ_8 if not otherwise specified.

4.1. Basic mechanism of the model

We start with an example which illustrates the basic mechanism of the algorithm Eqs. (15)–(17). Let us consider an elliptical initial shape (see dotted line in Fig. 2). If we take only the AC step Eqs. (15) and (16), then the initial shape shrinks under the motion by mean curvature (see dashed line) (Huisken, 1984). The position with a higher curvature moves faster than those with lower curvatures on the curve. However, with the mass correction step Eq. (17), the curve uniformly moves to the outward normal direction (see solid line). By continuing this process, the initial ellipse relaxes to the circular shape with the same mass.

4.2. Comparison of two models

To see the difference between two models Eqs. (4) and (6), we consider the following numerical experiments. On a computational domain $\Omega=[0,1]\times[0,1]$ with a mesh grid of 128×128, the initial conditions are given as (i) $\phi_{ij}=1$ if $40\leqslant i,\ j\leqslant 88$, (ii) $\phi_{ij}=1$ if $56\leqslant i,\ j\leqslant 72$, and $\phi_{ij}=0$ otherwise (see Fig. 3(a)). The temporal step size is chosen as $\Delta t=1.0\text{e}{-5}$.

Fig. 3(b) and (c) show the numerical results of Eqs. (4) and (6) at a steady state with two different initial conditions, respectively. Here, we define the numerical steady state as the state when the discrete l_2 norm of the difference between ϕ^{n+1} and ϕ^n becomes less than a given tolerance, $tol=1.0\text{e}{-6}$. Observing the numerical results in the top row of Fig. 3, we can see that both models work well when the initial feature is large enough. It should be noted that the order parameter in the outside phase is 0.009 for Eq. (4), on the other hand, the value is 0.0 for Eq. (6) with our proposed numerical scheme. The reason why the order parameters have different values is that our scheme corrects mass loss in the interfacial region. If the geometry is small, then the geometry disappears with Eq. (4) (see the second row of Fig. 3(b)). On the other hand, with our scheme, the drop stays as shown in the second row of Fig. 3(c).

Next, we present numerical simulations of three-dimensional cubes in Fig. 4. The initial conditions are given on $\Omega=[0,1]\times[0,1]\times[0,1]$ with $h=1/128$ as (i) $\phi_{ijk}=1$ if $40\leqslant i,\ j,\ k\leqslant 88$, (ii) $\phi_{ijk}=1$, if $56\leqslant i,\ j,\ k\leqslant 72$, and $\phi_{ijk}=0$ otherwise (see Fig. 4(a) for the isosurfaces $\phi=0.5$). The temporal step size $\Delta t=1.0\text{e}{-5}$ is used. Fig. 4(b) and (c) show the steady states with Eqs. (4) and (6), respectively. The three-dimensional results are almost similar to the two-dimensional ones.

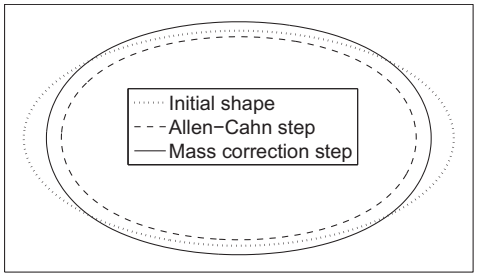

Fig. 2. Basic mechanism of the proposed numerical scheme.

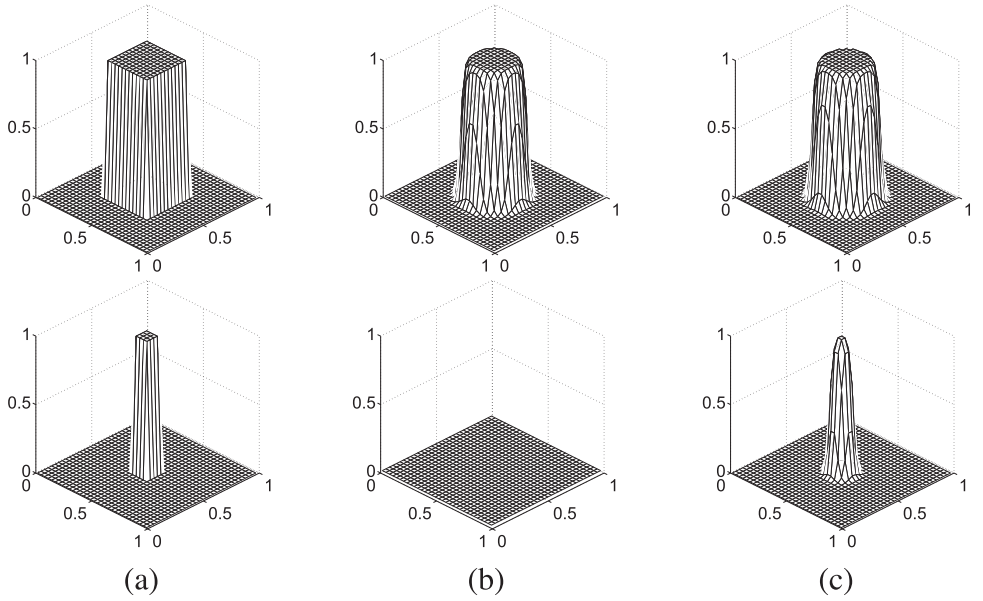

Fig. 3. (a) Initial conditions with two different shapes. (b) and (c) Are numerical results from Eqs. (4) and (6), respectively.

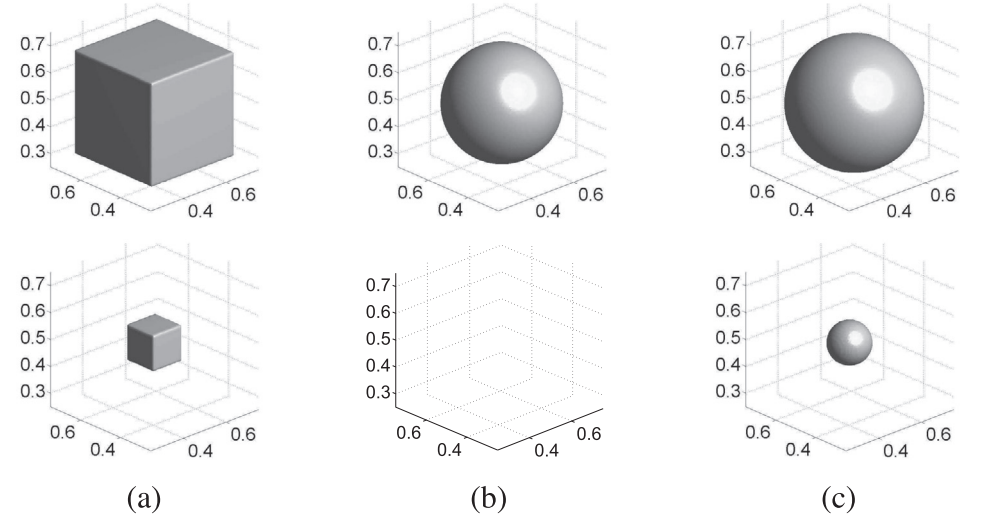

Fig. 4. (a) Two different-sized cubes for initial conditions. (b) and (c) Are numerical results from Eqs. (4) and (6), respectively.

4.3. Evolution of disks

In Bronsard and Stoth (1997), the authors gave the evolution law for radii of spheres in n-dimensional geometric flows. For the m interfaces of radii r_i for $i = 1, 2, \ldots, m$ with $r_j < r_{j+1}$ for $j = 1, 2, \ldots, m-1$, the equations of evolution in n-dimensional case are given by

$$\frac{dr_i}{dt} = (n-1)\left(\frac{\sum_{k=1}^{m} r_k^{n-2}}{\sum_{k=1}^{m} r_k^{n-1}} - \frac{1}{r_i}\right), \quad i = 1, 2, \ldots, m.$$

We consider two disjoint circular interfaces in two-dimensional space. Assume that the two interfaces have radii r and R with $r < R$, then the equations of evolution become

$$\frac{dr}{dt} = \frac{2}{r+R} - \frac{1}{r}, \tag{18}$$

$$\frac{dR}{dt} = \frac{2}{r+R} - \frac{1}{R}. \tag{19}$$

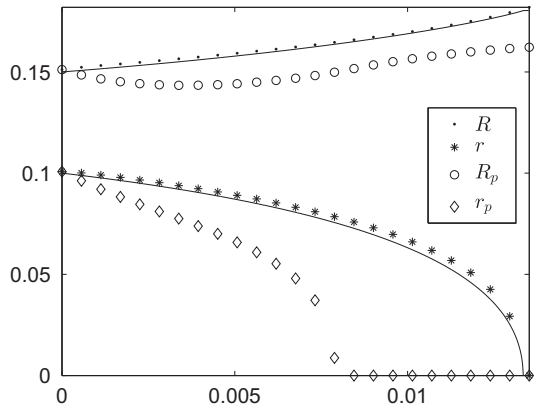

Fig. 5. Evolution of the radii of two distinct circles against time. R and r are radii from Eq. (6) and R_p and r_p are radii from Eq. (4). The solid lines are the corresponding reference solutions.

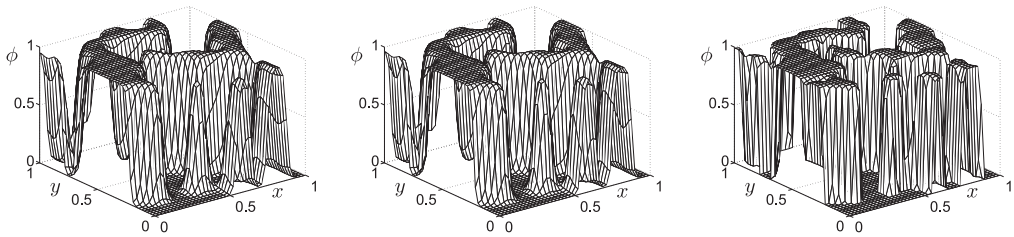

Fig. 6. Snapshots at the same time $T = 50h^2$ with three different time steps. The time steps are shown below each figure.

From the above equations, we can get the time t_f at which smaller circle disappears by solving a system of ordinary differential equations (Brassel & Bretin, 2011):

$$t_f = -0.5r_0R_0 + 0.25\left(r_0^2 + R_0^2\right)\ln\left(1 + \frac{2r_0R_0}{(R_0 - r_0)^2}\right), \tag{20}$$

where r_0 and R_0 are the initial radii. We present results for $r_0 = 0.1$ and $R_0 = 0.15$ using a temporal step size $\Delta t = 1.1264 \times 10^{-4}$ on $\Omega = [0,1] \times [0,1]$ with a mesh grid 128×128. Then $t_f = 0.0133$ by Eq. (20). For the reference solutions of r and R, we numerically solve the ordinary differential equations by using the fourth order Runge–Kutta method (Bhargava & Takhar, 2000; Burden & Faires, 2005; Zhao & Wei, 2013).

In Fig. 5, the solid lines represent the result from the Runge–Kutta method, dot and star represent the radius evolutions of R and r with Eq. (6), respectively, and circle and diamond also represent the radius evolutions of R_p and r_p with Eq. (4), respectively. As shown in Fig. 5, R grows monotonically with our numerical scheme and r disappears at the similar time as predicted from the analytic calculation. Compared to Eq. (6), the results from Eq. (4) do not predict the theoretical prediction because most mass diffuse into the bulk phase from a global mass conservative Lagrange multiplier.

4.4. Practically unconditional stability test

We perform a numerical experiment to demonstrate the practically unconditional stability of the proposed scheme. In this test, the initial condition is random perturbation around 0.5, i.e., $\phi(x,y,0) = 0.5 + 0.02\text{rand}(x,y)$, where $\text{rand}(x,y)$ is a random number between -1 and 1. We use a mesh grid size 128×128 on the computational domain $\Omega = [0,1] \times [0,1]$ with three different time steps, $\Delta t = 0.1h^2,\ h^2$, and $10h^2$. Fig. 6(a)–(c) are snapshots at the same time $T = 50h^2$ with three different time steps. These results suggest that the proposed scheme is practically unconditionally stable. We should note that the value of Δt is typically smaller than $0.1h^2$ to get accurate numerical approximations. Otherwise, the numerical scheme may unnecessarily result in large discretization errors. Therefore, the fact that we can use two orders of magnitudes larger time step than $\Delta t = 0.1h^2$ suggests the proposed scheme is practically unconditionally stable.

5. Conclusions

We presented a new numerical scheme for solving the conservative Allen–Cahn equation with a space–time dependent Lagrange multiplier. Rubinstein and Sternberg's nonlocal Allen–Cahn equation conserves mass. However, with their model it is difficult to keep small features since they dissolve into the bulk region because mass conservation is realized by a global correction using the time-dependent Lagrange multiplier. To resolve the problem, we used a space–time dependent Lagrange multiplier to preserve the volume of the system and proposed a practically unconditionally stable hybrid scheme to solve the model. We performed numerical experiments such as the basic mechanism of the model, a comparison with previous model, the temporal evolution of drops in two- and three-dimensional spaces, and a practically unconditional stability test of the proposed numerical scheme. The numerical results indicate a potential usefulness of our proposed numerical scheme for accurately calculating geometric features of interfaces. In particular, it is applicable to various problems with a mass conservation constraint.

Acknowledgments

The first author (J.S. Kim) was supported by a Korea University Grant. The corresponding author (Y. Choi) thanks Dr. D. Jeong and D. Lee for many useful discussions. The authors also wish to thank the reviewers for the constructive and helpful comments on the revision of this article.

References

Abels, H., Garcke, H., & Grun, G. (2012). Thermodynamically consistent, frame indifferent diffuse interface models for incompressible two-phase flows with different densities. *Mathematical Models and Methods in Applied Sciences, 22*.

Allen, S. M., & Cahn, J. W. (1979). A microscopic theory for antiphase boundary motion and its application to antiphase domain coarsening. *Acta Materialia, 27*, 1085–1095.

Aristotelous, A. C., Karakashian, O., & Wise, S. M. (2013). A mixed discontinuous Galerkin, convex splitting scheme for a modified Cahn–Hilliard equation and an efficient nonlinear multigrid solver. *Discrete and Continuous Dynamical Systems. Series B, 18*, 2211–2238.

Bates, P. W., & Jin, J. (2013). Global dynamics of boundary droplets. *Discrete and Continuous Dynamical Systems, 34*, 1–17.

Beneš, M., Yazaki, S., & Kimura, M. (2011). Computational studies of non-local anisotropic Allen–Cahn equation. *Mathematica Bohemica, 136*, 429–437.

Bhargava, R., & Takhar, H. S. (2000). Numerical study of heat transfer characteristics of the micropolar boundary layer near a stagnation point on a moving wall. *International Journal of Engineering Science, 38*, 383–394.

Brassel, M., & Bretin, E. (2011). A modified phase field approximation for mean curvature flow with conservation of the volume. *Mathematical Methods in the Applied Sciences, 34*, 1157–1180.

Briggs, W. L., & Steve, F. (1987). *A multigrid tutorial* (Vol. 72). Philadelphia: SIAM.

Bronsard, L., & Stoth, B. (1997). Volume-preserving mean curvature flow as a limit of a nonlocal Ginzburg–Landau equation. *SIAM Journal on Mathematical Analysis, 28*, 769–807.

Burden, R. L., Faires, J. D. (2005). Numerical Analysis, Cengage Learning, Belmont.

Cahn, J. W., & Hilliard, J. E. (1958). Free energy of a nonuniform system. I. Interfacial free energy. *The Journal of Chemical Physics, 28*(2), 258–267.

Heida, M., Malek, J., & Rajagopal, K. R. (2012). On the development and generalizations of Cahn–Hilliard equations within a thermodynamic framework. *Zeitschrift fur angewandte Mathematik und Physik, 63*, 145–169.

Heida, M., Malek, J., & Rajagopal, K. R. (2012). On the development and generalizations of Allen–Cahn and Stefan equations within a thermodynamic framework. *Zeitschrift fur angewandte Mathematik und Physik, 63*, 759–776.

Huisken, G. (1984). Flow by mean curvature of convex surfaces into spheres. *Journal of Differential Geometry, 20*, 237–266.

Kim, J. (2012). Phase-field models for multi-component fluid flows. *Communications in Computational Physics, 12*(3), 613–661.

Li, Y., Lee, H. G., Jeong, D., & Kim, J. (2010). An unconditionally stable hybrid numerical method for solving the Allen–Cahn equation. *Computers and Mathematics with Applications, 60*, 1591–1606.

Lowengrub, J., & Truskinovsky, L. (1998). Quasi-incompressible Cahn–Hilliard fluids and topological transitions. *Proceedings of Royal Society of London A: Mathematical, Physical and Engineering Sciences, 454*, 2617–2654.

Ma, J., Jiang, Y., & Xiang, K. (2009). Numerical simulation of blowup in nonlocal reaction–diffusion equations using a moving mesh method. *Journal of Computational and Applied Mathematics, 230*, 8–21.

Ren, X., & Wei, J. (2009). On a phase field problem driven by interface area and interface curvature. *European Journal of Applied Mathematics, 20*, 531–556.

Rubinstein, J., & Sternberg, P. (1992). Nonlocal reaction–diffusion equations and nucleation. *IMA Journal of Applied Mathematics, 48*, 249–264.

Stuart, A., & Humphries, A. R. (1998). *Dynamical systems and numerical analysis* (Vol. 2). Cambridge: Cambridge University Press.

Trottenberg, U., Oosterlee, C., & Schuller, A. (2001). *Multigrid*. London: Academic Press.

Ward, M. J. (1996). Metastable bubble solutions for the Allen–Cahn equation with mass conservation. *SIAM Journal on Mathematical Analysis, 56*, 1247–1279.

Ward, D. S. M. J., & Wetton, B. (2001). The dynamics of drops and attached interfaces for the constrained Allen–Cahn equation. *European Journal of Applied Mathematics, 12*, 1–24.

Xia, Y., Xu, Y., & Shu, C. W. (2009). Application of the local discontinuous Galerkin method for the Allen–Cahn/Cahn–Hilliard system. *Communications in Computational Physics, 5*, 821–835.

Yang, X., Feng, J. J., Liu, C., & Shen, J. (2006). Numerical simulations of jet pinching-off and drop formation using an energetic variational phase-field method. *Journal of Computational Physics, 218*, 417–428.

Yue, P., Zhou, C., & Feng, J. J. (2007). Spontaneous shrinkage of drops and mass conservation in phase-field simulations. *Journal of Computational Physics, 223*, 1–9.

Zhang, Z., & Tang, H. (2007). An adaptive phase field method for the mixture of two incompressible fluids. *Computers and Fluids, 36*, 1307–1318.

Zhao, S., & Wei, G. W. (2013). A unified discontinuous Galerkin framework for time integration. *Mathematical Methods in the Applied Sciences, 37*(7), 1042–1071.